Marine Geology 346 (2013) 310–325

Contents lists available at ScienceDirect

Marine Geology

journal homepage: www.elsevier.com/locate/margeo

Geomorphometry and processes that built Necker Ridge, central North Pacific Ocean

James V. Gardner [a,*], Brian R. Calder [a], Mashkoor Malik [b]

[a] Center for Coastal and Ocean Mapping, University of New Hampshire, Durham, NH 03824, USA
[b] Office of Ocean Exploration and Research, National Oceanic and Atmospheric Administration, Silver Spring, MD 20910, USA

ARTICLE INFO

Article history:
Received 1 May 2013
Received in revised form 4 September 2013
Accepted 14 September 2013
Available online 15 October 2013

Communicated by D.J.W. Piper

Keywords:
Necker Ridge
multibeam bathymetry
Mid-Pacific Mountains
volcanic flows
volcanic pinnacles
summit platform
archipelagic apron

ABSTRACT

Necker Ridge is an enigmatic 650-km long, narrow, linear aseismic bathymetric feature that rises 2500 to 3000 m above the abyssal seafloor south of the Hawaiian Ridge. The ridge is the largest of a series of aseismic ridges that emanate from the eastern side of the Mid-Pacific Mountains outward towards the northeast. The trend of Necker Ridge is at an angle to fracture zones and spreading centers in the region, so its origin is controversial, yet it is a major feature on this part of the Cretaceous Pacific Plate. The entire feature, from Necker Island on the Hawaiian Ridge to the eastern Mid-Pacific Mountains, including the adjacent abyssal seafloor, was mapped in 2009 and 2011 with the latest generation of multibeam echosounders. The detailed bathymetry shows the ridge to be constructed of a series of stacked, thick (200–400 m) volcanic flows that can be traced along the trend of Necker Ridge for 100 s of km. This continuity suggests that the volcanism erupted simultaneously along almost the entire length of the feature and not as spatially episodic areas of extrusion. Three relatively flat platforms occur on the summit region, presumably constructed of shallow-water carbonates when these portions of the ridge were at sea level. A conspicuous lack of thick pelagic sediment on the non-platform ridge summit and flanks is seen throughout the ridge. The lack of landslides along the length of the ridge is equally puzzling. The southern end of the ridge is connected by a saddle to the Mid-Pacific Mountains whereas the northern end of the ridge is buried by an archipelagic apron of the southern flank of the Hawaiian Ridge.

1. Introduction

Over the past decade large areas of the seafloor have been mapped using highly accurate latest-generation multibeam echosounders to provide data necessary for coastal states to make a case for an extended continental shelf under Article 76 of the U.N. Convention on the Law of the Sea. The U.S. effort to date has collected bathymetry and co-registered acoustic backscatter from more than two million km^2 offshore the U.S. regions of the Atlantic and Arctic Oceans, the Gulf of Mexico and Bering Sea and U.S. territories in the Pacific (Gardner et al., 2006). The large regional coverage of each of these data sets provides for the first time the ability to quantitatively describe large expanses of the seafloor that, until now, were only known in the most general terms. The present study presents the first complete high-resolution (100 m/pixel) bathymetric map of Necker Ridge (Fig. 1), a large, enigmatic seafloor feature in the central Pacific that has received little attention prior to this mapping. The new multibeam data allow a three-dimensional quantitative analysis (geomorphometry) of this seascape. 'Geomorphometry' is a term seldom used by the marine geology seafloor-mapping community when describing features of the seafloor, perhaps because the term is defined as the science of quantitative land surface analysis (Pike, 1995). However, the definition of geomorphometry, when the land reference is taken *senso lato*, accurately describes seafloor-mapping studies based on bathymetry data produced by multibeam echosounders. Consequently, the term geomorphometry has been used here. The focus of this paper is to use the geomorphometry of Necker Ridge to describe the present ridge and the processes that constructed and modified it.

2. Regional setting

Necker Ridge is a southwest–northeast-trending aseismic linear bathymetric high that spans 650 km from the Mid-Pacific Mountains on the southwest to the Hawaiian Ridge on the northeast (Fig. 1). Necker Ridge was constructed on the Pacific Plate in the Late Cretaceous but sits on mid Cretaceous oceanic crust (Müller et al., 1997). A back-track plot (Wessel and Kroenke, 1997) suggested that this part of the Pacific Plate formed at ~20°S and migrated northward across the equator to its present position at ~20°N (Thiede et al., 1981). The summit of the ridge varies in water depths from ~1500 to ~3600 m and the ridge rises 2500–3000 m above the adjacent abyssal seafloor. The width of the ridge varies from a maximum of 46.0 km in the south to less than 5.8 km in the far north. The northwest-facing flank of the ridge is generally steeper (~20°) than the southeast-facing flank (~10°). The ridge is primarily composed of stacked basalt flows and in three places

* Corresponding author.
E-mail address: jim.gardner@unh.edu (J.V. Gardner).

0025-3227/$ – see front matter © 2013 Elsevier B.V. All rights reserved.
http://dx.doi.org/10.1016/j.margeo.2013.09.014

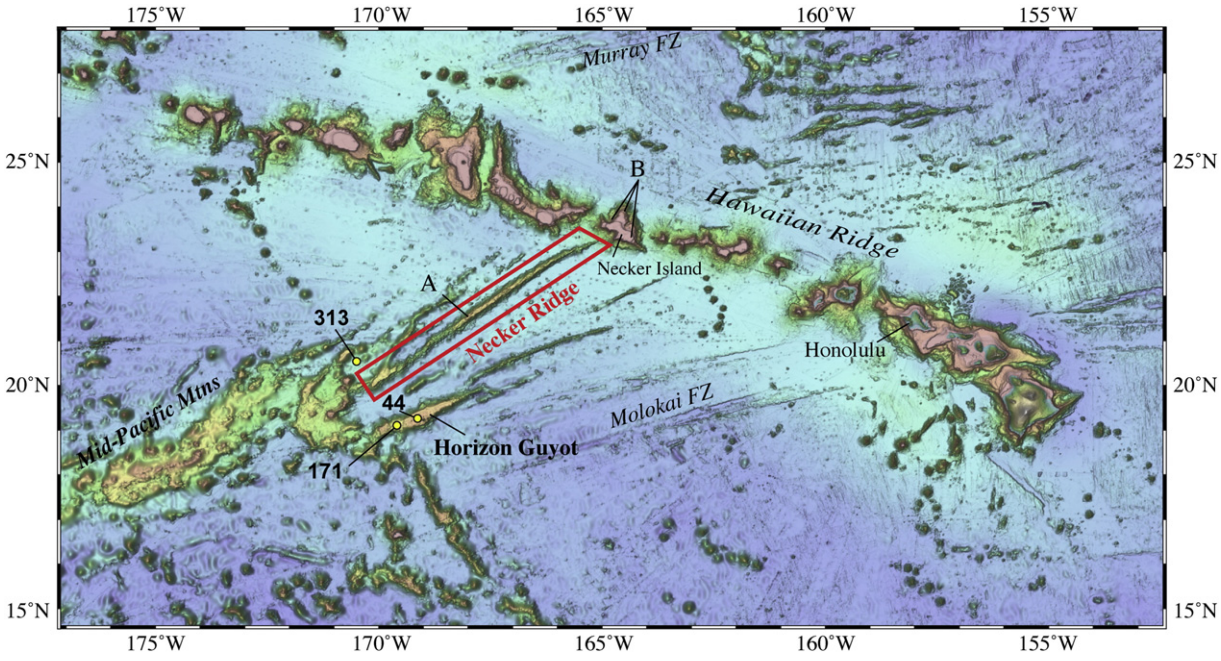

Fig. 1. Location map of Necker Ridge (red polygon). Bathymetry from Ryan et al. (2009). Sample sites: yellow circles DSDP sites; A — Saito and Ozima (1977); B — Dalrymple et al. (1974) and Clague and Dalrymple (1975). (For interpretation of the references to color in this figure legend, the reader is referred to the web version of this article.)

is topped with what appear from their morphologies to be shallow-water carbonate platforms that are buried by a blanket of pelagic sediments. The three large, roughly flat-topped areas of Necker Ridge (called here South Saddle, North Platform and South Platform) are shallower than ~2650 m. South Saddle is a 14-km long section at the junction of Necker Ridge and the Mid-Pacific Mountains whereas South Platform is a 70 km long section in the southwest region of Necker Ridge and North Platform is a 165-km long section in the northeast (Fig. 2).

The origin of the ridge has been debated since the 1970s. Rocks dredged from Necker Ridge were dated at 82.5 Ma (Saito and Ozima, 1977). Rocks from Necker Island, near the junction of Necker Ridge and the Hawaiian Ridge (Fig. 1), were dated at ~10 Ma by Dalrymple et al. (1974) although an unusual fresh rhyolite porphyry from the island was dated at ~71 Ma (Clague and Dalrymple, 1975). Rocks dredged from the northwest flank of Necker Island were dated at ~77 Ma (Clague and Dalrymple, 1975), which suggested to them that part of Necker Island may be an isolated Pacific Plate seamount that was incorporated into the Hawaiian Ridge as that portion of the plate migrated over the Hawaiian hot spot. Atwater et al. (1993) showed from marine magnetic anomalies that the adjacent oceanic crust was formed within the Cretaceous Quiet Zone that spans from 119 to 83 Ma. The trend of Necker Ridge is oblique to the trends of the nearby Murray and Molokai Fracture Zones (Fig. 1), suggesting that the ridge is not related to either fracture zone. The only suggestion that the strike of Necker Ridge may continue to the northeast through Necker Island and beyond is a brief statement in a description of Necker Island that mentioned "Numerous dikes on the island trend northeast–southwest and have nearly vertical dips" (Dalrymple et al., 1974, p. 730). Bridges (1997) observed that the trends of some seamounts southeast of the Hawaiian Ridge are parallel to the Necker Ridge trend, which suggests that the seamounts may be related to the same conditions as Necker Ridge; i.e., Necker Ridge may have formed by regional mid-plate volcanism. DSDP Site 171, on a saddle of Horizon Guyot to the immediate south of Necker Ridge (Fig. 1), recovered a Late Cretaceous volcanic basement beneath a predominately shallow-water carbonate section but the section also provides evidence that volcanism resumed for at least 5 Ma to as long as 30 Ma after the initial volcanism (Winterer et al., 1973). A reoccurrence of volcanism at this same time is also indicated at DSDP Site 313 in the nearby Mid-Pacific Mountains (Larson et al., 1975).

The three large elongate, roughly flat-topped platforms occur on the crest of Necker Ridge (Fig. 3) and resemble the somewhat elongated

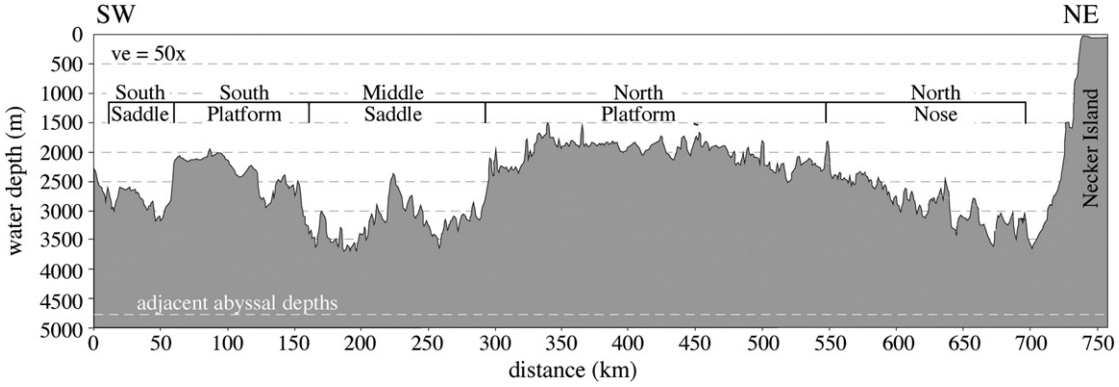

Fig. 2. Bathymetry profile down crest of Necker Ridge. The white dashed line is the general depth (4650 to 4850 m) of the adjacent abyssal seafloor.

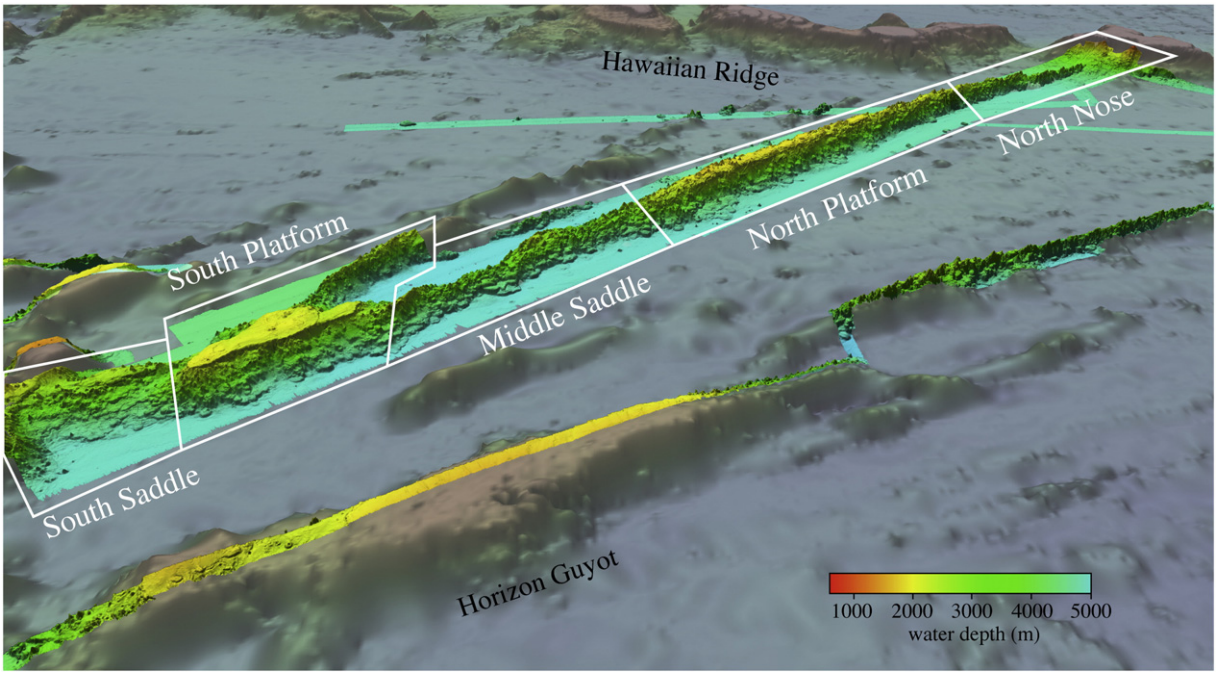

Fig. 3. Perspective view of Necker Ridge new multibeam bathymetry overlain on Global Multi-Resolution Topography (Ryan et al., 2009). White polygons define areas discussed in text. (For interpretation of the references to color in this figure legend, the reader is referred to the web version of this article.)

platforms of Horizon Guyot located 120 km south of Necker Ridge, as well as the more typical circular guyots that are found in the nearby eastern Mid-Pacific Mountains (Fig. 1). The process that is generally invoked to have formed the truncated top of a seamount (guyot) or ridge is erosion at sea level and then subsequent subsidence (Hess, 1946; Hamilton, 1956; Menard, 1984; Winterer and Metzler, 1984). However, as was pointed out by Winterer and Metzler (1984), the details of subsidence, emergence and renewed subsidence of the Mid-Pacific Mountains, and presumably nearby Necker Ridge and Horizon Guyot, are much more complicated. The range of dated rocks from Necker Island, as well as the complicated history at nearby Horizon Guyot and the Mid-Pacific Mountains, attests to a potential complicated history of Necker Island and leaves any genetic relationship between Necker Island, the Hawaiian Ridge and Necker Ridge an open question.

3. Data and methods

Four cruises collected multibeam data on transits that crossed Necker Ridge with a single multibeam-echosounder (MBES) swath and one cruise ran a line down the length of the ridge, again with a single MBES swath (Table 1). Two of these older crossings (in 1985 and 2000) were made with first- or early-generation multibeam systems that did not collect high-quality data; however, the two crossings in 2009 were collected with much newer-generation systems that collected high-quality data. A third multibeam line was run down the crest of Necker Ridge but, again, used an early-generation MBES. The previous multibeam data do not provide any sense of the details of the morphology of Necker Ridge. Predicted bathymetry from satellite altimetry (Smith and Sandwell, 1997 v. 14.1) and the Global Multi-Resolution Topography (GMRT) compilation (Ryan et al., 2009 v. 2.4) provides a gross view of the ridge but at a spatial resolution of ~1850 m/pixel. Most of the data used in this report were collected on two dedicated mapping cruises with the latest generations of Kongsberg Maritime MBES systems that collected high-quality bathymetry and co-registered acoustic backscatter at 30 to 50 m sounding spacings in the water depths of Necker Ridge.

Table 1
Cruises that collected multibeam data on Necker Ridge.

Cruise ID	Year	Multibeam system	Comments
RC2610	1985	Seabeam Classic	Single crossing
AVON01MV	1999	Seabeam 2000	Single crest profile
NECR004RR	2000	Seabeam 2100	Single crossing
KM0908	2009	Kongsberg EM 120	Single crossing
KM0913	2009	Kongsberg EM 120	Single crossing
EX0909	2009	Kongsberg EM 302	Horizon Guyot and MPM[a]
KM1121	2011	Kongsberg EM 122	Complete coverage

[a] Mid-Pacific Mountains.

The data used to construct the digital terrain model (DTM) of the entire Necker Ridge, its flanks and adjacent areas of the abyssal seafloor (Fig. 3) are from the 2009 and 2011 MBES cruises. Most of the data were collected during two cruises that spent 16 days mapping Necker Ridge; a 2009 cruise of the NOAA Ship *Okeanos Explorer* (EX0909) that used a 30-kHz Kongsberg Maritime EM 302 MBES and a 2011 cruise of the RV *Kilo Moana* (KM1121) equipped with a 12-kHz Kongsberg Maritime EM 122 MBES. The EM302 MBES system has a $1° \times 1°$ (transmit and receives) array and the EM122 MBES has a $1° \times 2°$ array. Both MBES systems incorporate transmit beam steering up to $\pm 10°$ from vertical to compensate for pitch, roll compensation up to $\pm 10°$ and perform yaw corrections by separating the array into a series of en echelon sectors. The beam footprints (on a flat bottom) of both MBES systems at these water depths are ~35 m. A full patch test was performed in deep water immediately prior to each cruise, including a conductivity–temperature–depth cast to calibrate the shipboard expendable bathythermographs (XBTs). A total of 86 XBTs were cast during the two cruises so that accurate sound-speed profiles of the water column could be calculated and used to perform ray tracing of individual soundings. Cross-line checks were used to determine that the depth precision across the swath of both systems was better than 0.5% of water depth. Navigation from both cruises was by differential GPS and provided location uncertainties of about ± 2 m for each sounding. One of the three additional MBES lines (KM0913) was collected with a Kongsberg Maritime 12-kHz EM 120 MBES, the immediate predecessor of the EM 122. The other two lines (AVON01MV and NECR004RR) were collected with much older second-generation MBES systems (Seabeam 2000 and Seabeam 2100, respectively).

The senior author processed all of the raw data from the four 2009 and 2011 MBES cruises and generated a DTM for each cruise. When viewed together, the four DTMs showed no join artifact. This confirmed that no static shifts occurred between the four DTMs so the four data sets were combined into one DTM. The 1985, 1999 and 2000 Seabeam MBES lines all show large (>100 m) variable depth offsets from the four Kongsberg DTMs so these earlier data were not used to generate the final DTM.

After processing the data, individual soundings were extracted as ASCII xyz (longitude–latitude–depth) records and gridded using a 3-pixel weighted moving average algorithm (Ware et al., 1991). The DTM was constructed in geographic coordinates (degrees) referenced to the WGS84 ellipsoid. All depths are in corrected meters with respect to instantaneous sea level.

The DTM was gridded at 100-m/pixel because of the large range in water depths (<2000–5000 m) and the sounding spacing of the MBES data (~35 m) at the deeper water depths. The grid spacing generates some degree of smoothing of features at scales of >100 m.

The volumes cited in the text were calculated by reducing the ridge to a series of truncated rectangular pyramids with the basal plan and summit plan dimensions and heights of the ridge summits above their base and rounding down the sum to the nearest 500 km^3 to be conservative.

4. Results

4.1. Geomorphometry of Necker Ridge

Necker Ridge comprises a pile of stacked volcanic flows with a volume of 35,500 km^3 above the sediment surface and an unknown buried volume. Volcanic flows of Necker Ridge are identified in the MBES bathymetry data by their general lobate rough morphology and high acoustic backscatter (−20 dB) compared to the smooth surface and low acoustic backscatter (−33 to −37 dB) of the local sediments. The flow fronts morphologically resemble those pictured by Glass et al. (2007) from the submarine flanks of the western Galapagos. The volcanic flows were extruded along a narrow, linear NE–SW trend that strikes for the most part at 232° to the SW from the Hawaiian Ridge. Necker Ridge is capped in three places by relatively thick platforms that resemble the carbonate platforms of nearby Horizon Guyot. The ridge rises as much as 1.9 km above the abyssal seafloor to water depths that range from ~3600 to ~1500 m along its length. A profile along the summit of Necker Ridge (Fig. 2) shows the distinct morphological characteristics of the areas of saddles and platforms and the plunging northern terminus. For the purpose of description, Necker Ridge is subdivided into 5 sections (Figs. 2 and 3) based on the morphological characteristics of the summit region. South Saddle section is a narrow, relatively low-lying area with more than a third of its entire length covered by a relatively flat summit. It extends between the higher standing South Platform section to its northeast and the eastern Mid-Pacific Mountains to its southwest. The South Platform section is an elongated, relatively flat summit region on the southwestern section of Necker Ridge. The Middle Saddle section is another relatively low-lying area with a rugged summit that separates the South and North Platform sections. The North Platform section is a narrow elongate region that is mostly relatively flat but has areas of rough bathymetry. The North Nose section is a relatively low-lying area with a rugged summit that plunges to the northeast and spans the area between the North Platform and the archipelagic apron of Necker Island. Volcanic flows can be seen along both flanks of the entire structure, although the gentler slope of the south side shows the flows best (i.e., Fig. 4). In addition to the stacked volcanic flows, there are numerous small conical pinnacles, some rising as individual pinnacles and some interconnected in a somewhat sinuous fashion that are scattered on the flanks and tops of the seascape. Very few of the pinnacles are cratered although a few relatively large cratered cones with caldera diameters as large as 3 km occur on the abyssal seafloor immediately to the north and south of the ridge in the northern part of the area.

4.2. South Saddle section

The South Saddle (Figs. 3 and 4) is a 50 km long and 33 km wide section with the shallowest water depths of ~2650 m. The section trends N70E, 18° off the main trend of Necker Ridge, from a connection 15 km north of the southwestern nose of the South Platform section. Water depths on the south flank are 4850 m at the base of the section where it merges with abyssal depths, whereas the base on the north flank is at 4280 m depth. This difference in base depths must reflect the influence of deposition of material eroded from the adjacent bathymetric highs of the eastern Mid-Pacific Mountains that rise to the immediate north and northwest of the South Saddle section but not on the south side. The upper 515 m of the southeast-facing flank has a consistent slope of 24° whereas the lower 1430 m of this flank has a slope of <4° in contrast to the northwest-facing flank that has slopes that range from 21° to 30° throughout its entire extent. A 36-km long, relatively flat platform outlined by the 2850-m isobath (Fig. 4) occupies the southern two-thirds of the crest. An elevated region rises about 100 m above the 2850-m platform. The northern third of the summit of South Saddle is relatively sharp crested with northwest-facing slopes of ~16° and southeast-facing slopes of ~8°.

The bathymetry shows that this section of the ridge is composed of a series of at least 8 major stacked volcanic flows that are especially apparent on the southeast-facing slope (Fig. 4). The flow fronts vary in thickness from 200 to as much as 400 m with frontal slopes of 17° to 28°. The exposed upper surfaces of the major flows have slopes of less than 0.5°. Only flow 5 on the northwest-facing side can be correlated by water depth with flow 5 on the southeast-facing side of the saddle. The northwest-facing flank, which lacks any relief indicative of stacked volcanic flows other than basal flow 5, plunges to abyssal depths with a slope of ~22°.

Numerous isolated pinnacles of probable volcanic origin ring the southern edges of the South Saddle section although relatively small pinnacles occur scattered throughout the section (Fig. 5). The pinnacles show no particular correlation with shallower or deeper areas or proximity to the Mid-Pacific Mountains or to the adjacent South Platform section. A few scattered pinnacles are also found on the nearby abyssal seafloor on both sides of the section but with a much lower abundance than is found within the South Saddle section. The pinnacles stand in relief from less than 80 m to more than 400 m high, although most of them are 100–200 m high. Most of the pinnacles are conical in shape, although a few have an oval plan shape and none of them appear to be cratered at the resolution of the MBES. A few of the pinnacles have flat summits but these pinnacles are typically deeper than the ridge summit.

4.3. South Platform section

South Platform (Figs. 3 and 6) is a section of Necker Ridge that has a relatively large, teardrop-shaped, roughly flat-topped platform developed on the summit. This flat-topped feature is not called a guyot because it did not form on a single, or even coalesced seamount but instead is a relatively flat summit area that was constructed on part of a long, linear ridge. The South Platform section represents ~7900 km^3 of volcanic flows and sediment above the present abyssal seafloor that covers an area of 3050 km^2 of which 865 km^2 is covered by the flat-topped platform. This section of the ridge has a 57 km NE–SW length and a width of 22 km in the northern quarter tapering to 5.2 km at the southern end. The platform surface has ~150 m of local relief (Fig. 6 lower), with a mean water depth of 2115 m. This part of Necker Ridge stands 2280 m above the abyssal depths on the north flank and rises 2900 m on the south. This difference in relief is again probably because of deposition of material eroded from the Mid-Pacific Mountains to the

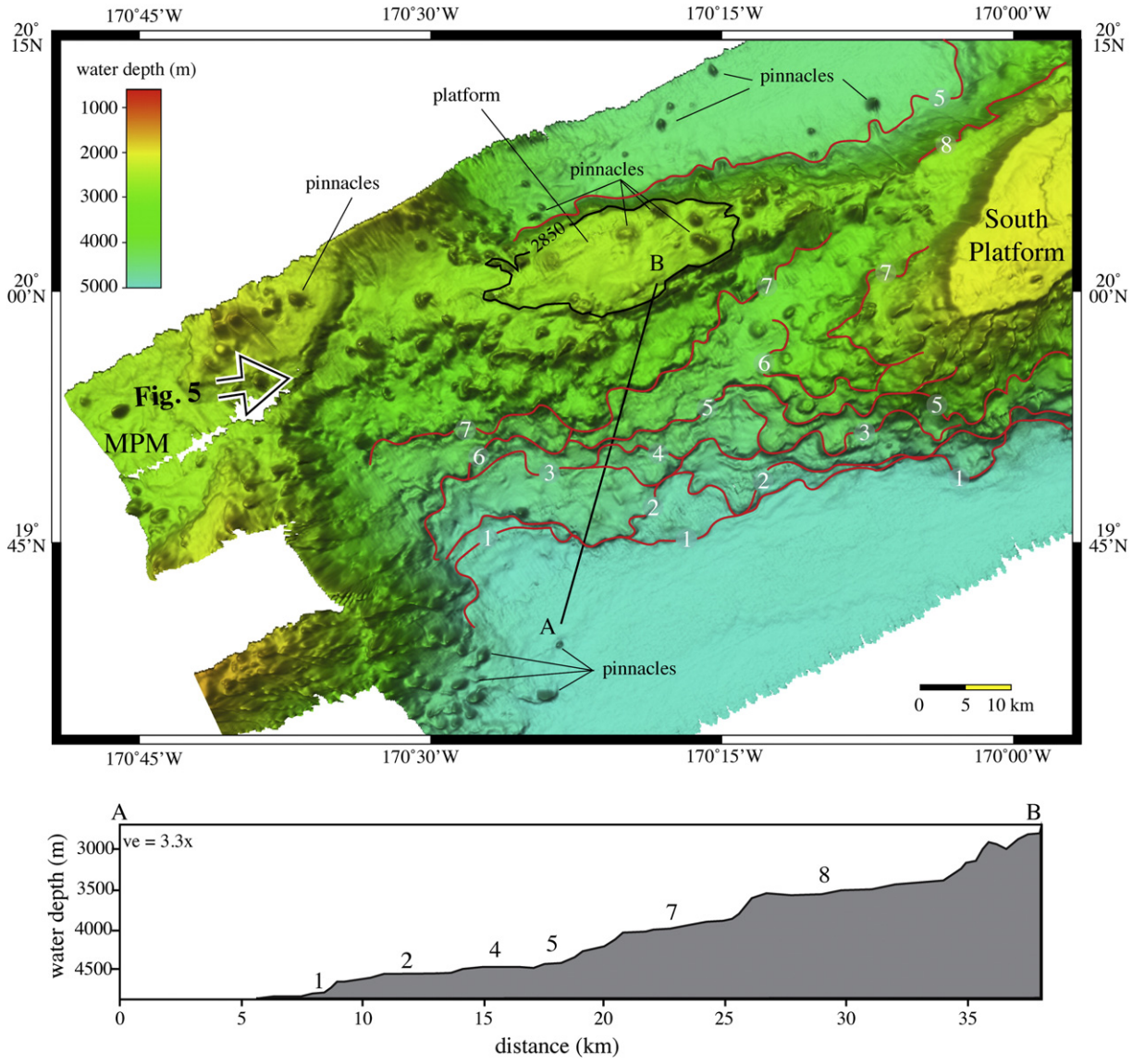

Fig. 4. Map view of bathymetry of South Saddle. Solid black polygon is the 2700-m isobath that outlines the upper platform. Red numbered lines trace the termini of volcanic flows. Numbers refer to sequence of flows from oldest to youngest. Profile A–B in lower panel shows the step-like nature of the numbered volcanic flows. The view direction of Fig. 5 is shown by open arrow. (For interpretation of the references to color in this figure legend, the reader is referred to the web version of this article.)

north side. The upper 700 + m of the flanks has relatively smooth slopes of >25°, similar to values measured by van Waasberger and Winterer (1993) on western Pacific guyots, but the lower part of the southeast-facing flank descends in a stair-step fashion of stacked volcanic flows with an overall slope of about 15°. The northwest-facing flank below the upper 700 + m is much less stair-stepped with relatively smooth slopes of ~20°. The upper ~700 m of the platform appears not to have been constructed by volcanic flows that formed the lower flanks. A NE–SW profile of the long axis of the platform (Fig. 6 lower) shows a large depression with more than 200 m of relief in the middle of the platform. The surface of the depression is rimmed by depths ~80 m shallower than the depression floor on all but an 8 km gap in the middle of the western side. The depression and the area of the platform just south of the depression are tilted to the NW at a 2.6° angle towards a breach or gap in the outer rim of the platform. The depression and surrounding rim are common features of drowned atolls (van Waasberger and Winterer, 1993). The northeastern end of the summit platform has a 110 m step-down to a NE–SW-elongated dome-shaped platform (Lower Platform), the highest point of which is ~300 m deeper than that of the water depth of South Platform. The relationship between Lower Platform and South Platform has some morphological similarity to that of terraces found along the edges of submarine rift zones of Hawaiian volcanoes (Moore et al., 1990; Eakins and Robinson, 2006), although the Hawaiian terraces were inferred to be related to the growth and subsidence of shield volcanoes.

Four of the numbered flows can be followed from the South Saddle section to the South Platform section (Fig. 6). Flows 1, 2 and 3 can confidently be followed along the southeast-facing flanks from South Saddle to the South Platform sections. Flows 5 and 8 on the northwest-facing lower flank of South Saddle can be continued from the South Saddle section but only flow 8 on the southeast-facing flank of South Saddle traces to the northwest-facing flank of the South Plateau section. Identification of flow 8 on the southeast-facing flank of South Plateau is problematic.

Only 7 pinnacles occur on the summit platform, some of which are isolated and others are clumped together (Fig. 6) although pinnacles are common and randomly scattered on the flanks of the South Platform section (Fig. 7). The platform pinnacles are generally conical in shape and rise 90–180 m above the general platform surface but none of the platform pinnacles have a truncated or cratered top. The pinnacles on the flanks are also conical in shape and typically have less than 150 m of relief. There is a higher density of flank pinnacles on the south- and

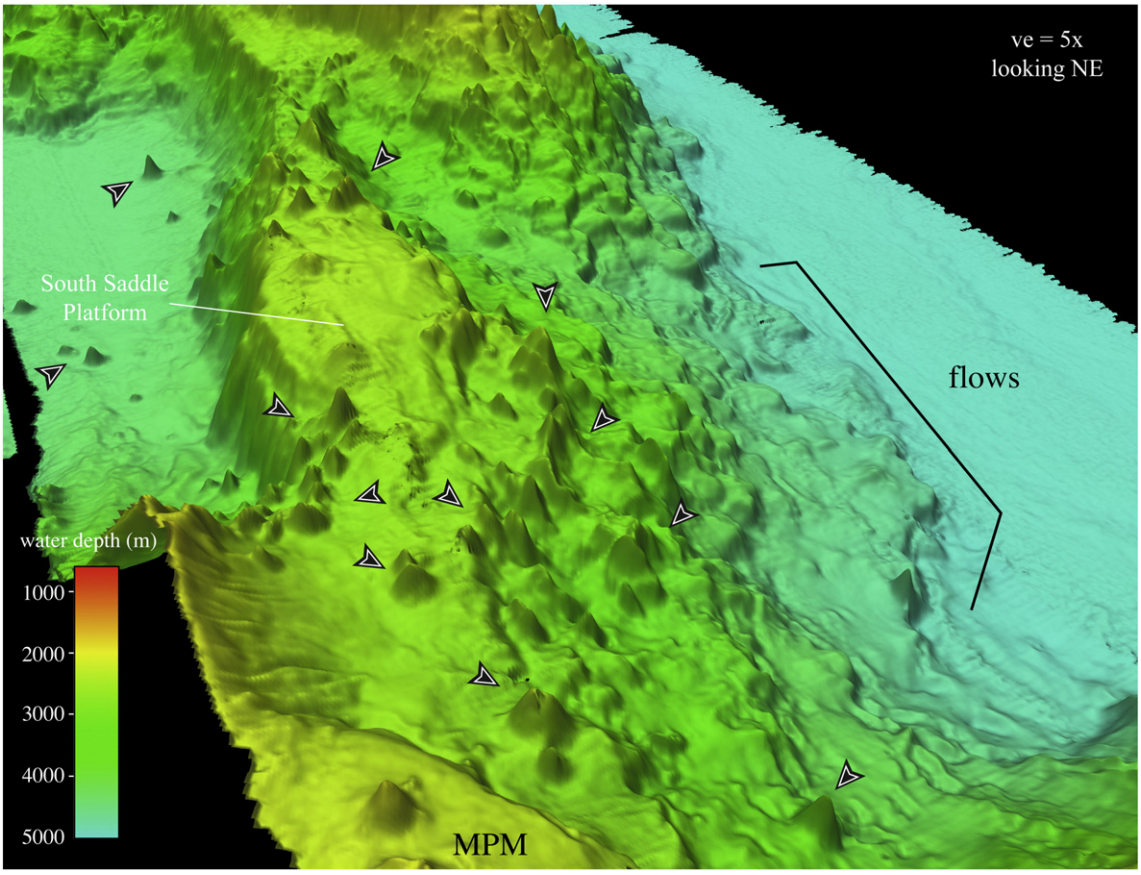

Fig. 5. Perspective view (looking NE) of South Saddle bathymetry showing the upper platform, scattered pinnacles (denoted by arrows) and volcanic flows. (For interpretation of the references to color in this figure legend, the reader is referred to the web version of this article.)

southeast-facing flanks of the South Platform section than on the other flanks. No pinnacles occur on Lower Platform.

Water depths of a sharp break in slope along the platform edge, from the relatively flat platform surface to the upper flanks (i.e., slope break or break depth), show an inconsistent relationship along the length of the South Platform section (Fig. 8A and B). The slope break is a parameter used to identify the depth of the lip of a guyot and is related to the point where sea level eroded the guyot surface (Vogt and Smoot, 1984; van Waasberger and Winterer, 1993). However, a slope break on a platform can also reflect the edge of a drowned shallow-water carbonate reef (Mark and Moore, 1987; Moore, 1987; Moore and Campbell, 1987). The depth of the slope break on the south side of South Platform is consistently ~50 m shallower than a corresponding point across the platform on the north side except for the region of the 200-m depression. North of the depression, the south side of the plateau is anywhere from 25 to 150 m shallower than on the north side. The slope break along the Lower Platform shows no consistent pattern (Fig. 8B).

A narrow sharp-crested connected ridge, called here North Arm, trends to the northeast at an angle of 15° to the trend of the Necker Ridge (Figs. 6 and 9). North Arm is 15 km wide at its widest and has slopes from 15–25° on both flanks. The ridge appears to be a series of extrusive volcanic rocks but lacks the distinct flow character seen in the South Saddle and South Platform sections. A 17-km-long saddle separates the prominent ridge from the South Platform section. Water depths of the saddle range from 3450 to 3530 m whereas the crest of North Arm lies in water depths of 2100–2700 m. Only 30% of North Arm was mapped with MBES; the remainder is resolved only in the ~2 km resolution of the predicted bathymetry and GMRT grids. However, it is clear from the global bathymetry grids that the arm has a 7.5 km offset to the north and then continues for another 130 km paralleling the main trend of Necker Ridge (Fig. 9).

4.4. Middle Saddle section

The Middle Saddle section (Figs. 3 and 9) is a 144-km-long segment of Necker Ridge with summit water depths that range from 2400 to 3900 m with an average water depth of ~3300 m. This section varies in width from 13 to 28 km and rises about 2.5 km above the abyssal seafloor. The northern flank has slopes of 15–30° whereas the southern flank has slopes generally less than 15°. The summit has a more rounded cross section than does North Arm or the South Saddle section although the surface of Middle Saddle is very rough with persistent relief of more than 100 m. Like the South Saddle and South Platform sections, the Middle Saddle section is constructed of a series of stacked volcanic flows, four of which (flows 1, 2, 3 and 4) can be followed from the southeast-facing flank of the South Platform section. Flows 1, 2, 3 and 4 on the northwest-facing flank can be correlated by depth to flows on the southeast-facing flank. The flows are as much as 300 m thick with 15–20° slopes of the flow fronts.

A strong bathymetric cross grain occurs on the southern half of the Middle Saddle section (Fig. 9). The trend of the cross grain is N30E, about 26° counterclockwise from the trend of Necker Ridge and it parallels the trend of the southern 23 km of North Arm that branches off of the South Platform section. However, the cross grain trend does not parallel the offset trend in North Arm. The northern half of the Middle Saddle section lacks the cross grain trend and the segment parallels the regional trend of Necker Ridge.

4.5. North Platform section

The North Platform section of Necker Ridge (Figs. 3 and 10), bordered on the south by the Middle Saddle section and on the north by the North Nose section, is the third region of Necker Ridge with a large, relatively flat but irregular summit platform. The North Platform section encompasses

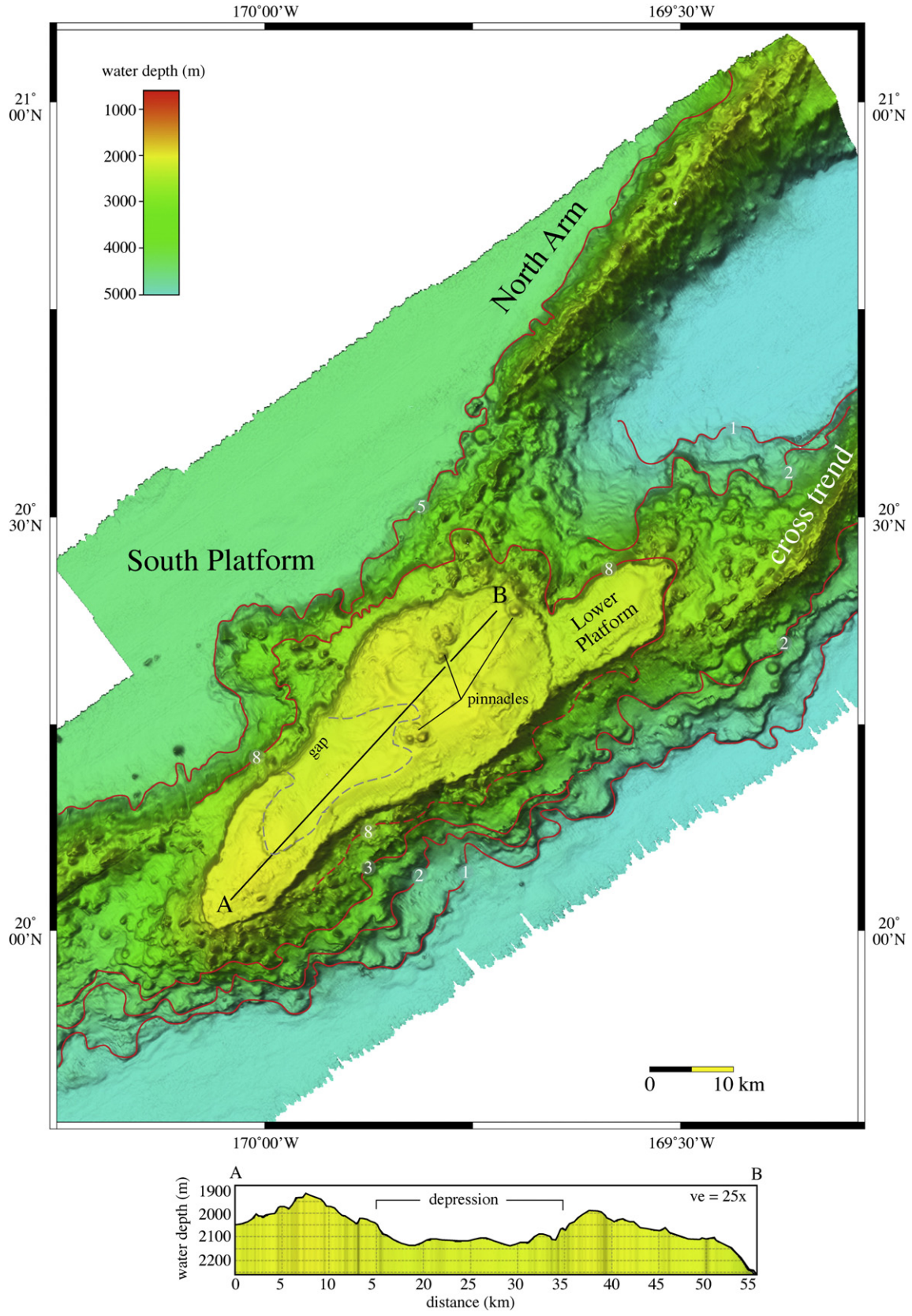

Fig. 6. Map view of bathymetry of South Platform and North Arm. Lower Platform. Red numbered lines show extent of volcanic flows. The numbering continues from those in Fig. 4. (For interpretation of the references to color in this figure legend, the reader is referred to the web version of this article.)

an area of 2285 km^2 and stretches NE–SW for 290 km. The width of this section ranges from 46 km at its widest to 19 km on its northern end. Summit water depths of the North Platform range from 1800 to ~2500 m. The summit platform has a considerable amount of relief (Fig. 10) with a mean depth of 1944 ± 268 m (2σ). The depths of the slope break of the summit platform tend to be 50 to 100 m

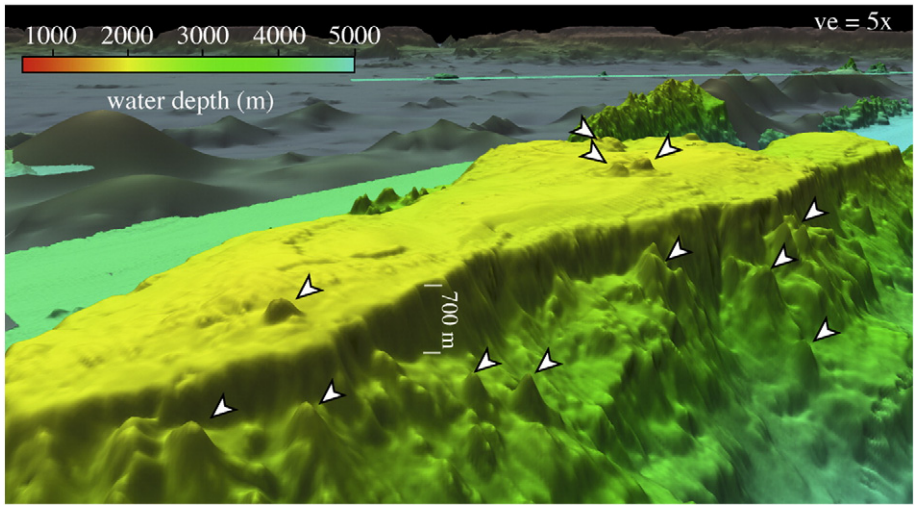

Fig. 7. Oblique view of bathymetry of South Platform. White arrowheads point to pinnacles. Typical thickness of platform above exposed volcanic flows is ~700 m. (For interpretation of the references to color in this figure legend, the reader is referred to the web version of this article.)

higher on the northwest-facing side (Fig. 8C and D). Unlike the South Platform section, the slope breaks of the North Platform section show a slight tendency to be deeper on the northwest-facing side relative to the southeast-facing side in shallower platform depths but are shallower in the deeper platform depths. The upper 500 to 700 m of the flanks of the relatively flat summit platform has slopes of 15° to 20° and the southeastern flank shows well-defined stacked volcanic flows compared to the northwestern flank. The lower flanks have slopes

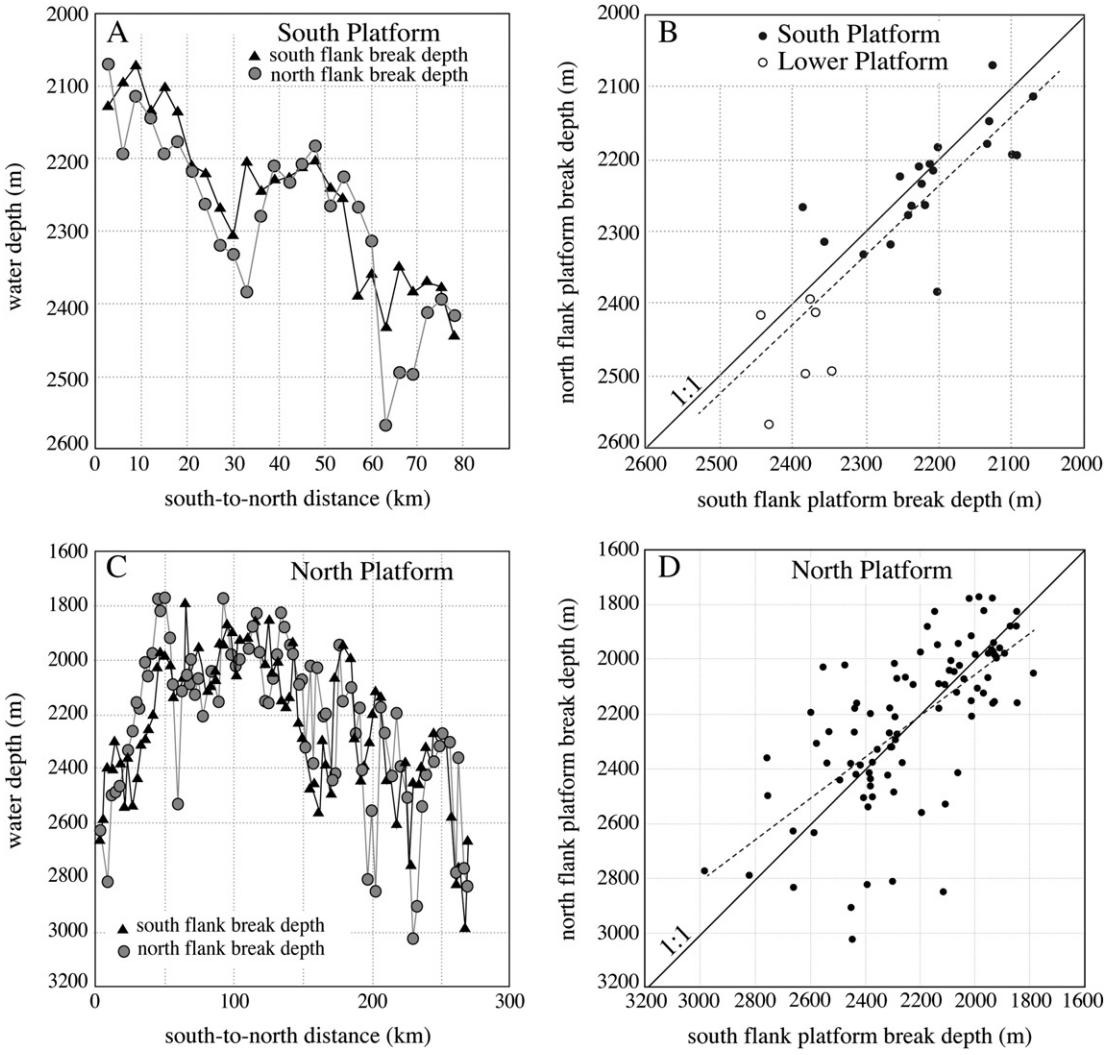

Fig. 8. Plots of depth of slope breaks on northwest- and southeast-facing flanks of North and South Platforms. Note the asymmetric nature of break depths on adjacent sides along the trend of the platforms.

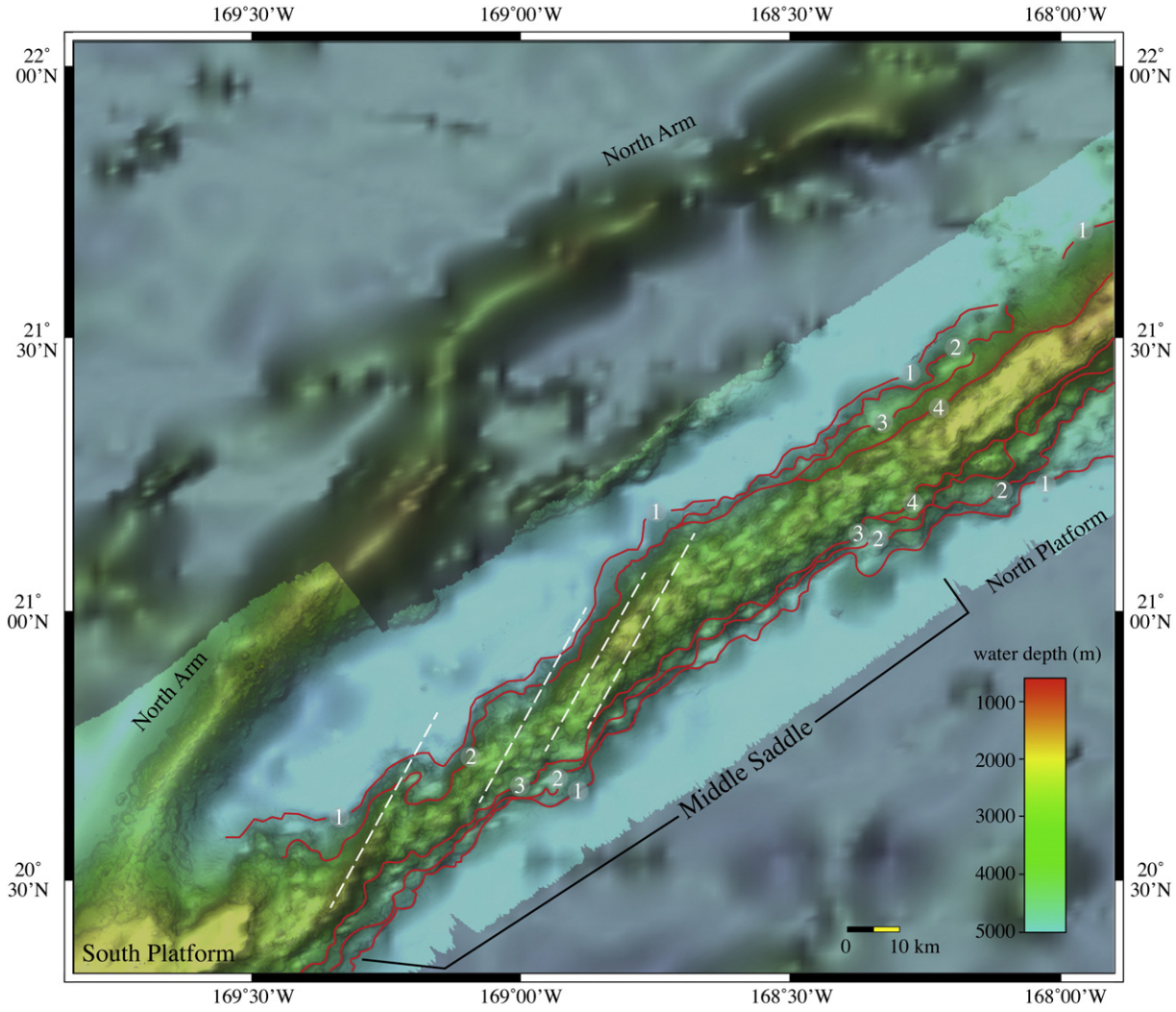

Fig. 9. Map view of bathymetry of Middle Saddle. Red numbered lines show extent of volcanic flows. The numbering continues from those in Fig. 6. Cross trend that parallels southwestern-most North Arm is indicated by white dashed lines. (For interpretation of the references to color in this figure legend, the reader is referred to the web version of this article.)

of 6° to 18° with neither flank being generally steeper than the other. Just as is found throughout most of Necker Ridge, the volcanic flows can be correlated with flows of the southern sections (Fig. 10A). Flows 1, 2, 3 and 4 can be correlated on the southeast-facing flank but only flows 1 and 4 can be correlated with any confidence on the northwest-facing flank. This implies that flows 2 and 3 may have extruded out only to the south and east, and did not spread out along both sides of the growing ridge as did flows 1 and 4.

Numerous pinnacles with slopes of ~25° rise as much as 400 m above the summit surface (Fig. 11). The largest pinnacles are found on the summit platform but numerous pinnacles also are present on the southern flank. The pinnacles range in plan shape from circular to elongate, some coalesced together, whereas others are individual features and none have a truncated top indicative of a guyot. The pinnacles typically appear grouped together; i.e., there are areas that have numerous pinnacles that are separated by areas with few or no pinnacles.

The base of the southern half of the North Platform section has several areas of flows that extend as much as 20 km out onto the abyssal floor; one area covers 400 km^2 and several other areas cover ~200 km^2. A large landslide scar (~150 km^2) on the north side of the southern section, directly opposite the landslide deposit (Fig. 10A), has carved out a 15 km wide scar and has eroded the entire vertical section of the ridge and summit platform. The landslide scar superficially resembles those described by Chadwick et al. (2008), although the scars they mapped were found on shallow (300–500 m water depths) volcanic cones on the northern Kermadec Arc. The landslide deposit on the abyssal seafloor covers an area of at least 180 km^2 and is as much as 100 m thick. Several large blocks of kilometer dimensions are scattered throughout the landslide deposit. This is the only landslide imaged in the MBES data along the entire length of Necker Ridge.

A step-down to the southwest in the depth of the seafloor occurs along a NW–SE trend centered at ~21°28′N/168°W (Fig. 10B). The abyssal seafloor descends ~400 m from depths of ~4500 m northeast of the above point to ~4900 m southwest of the step-down (Fig. 10B profile A–A′). The southern abyssal seafloor (Fig. 10B profile C–C′) drops only 100 m, from ~4800 m northeast of the point to ~4900 m southeast of the point. There is a corresponding ~500 m drop to the southwest in the summit platform water depths that occur roughly at this same point (Fig. 10B profile B–B′). The step-down occurs at the location of the large landslide described above.

4.6. North Nose section

The North Nose section of Necker Ridge is ~110 km long before its crest descends from ~2600 m to 3505 m water depths and is buried under the archipelagic apron of Necker Island (Figs. 3, 12 and 13). Abyssal depths seaward of the archipelagic apron of Necker Islands

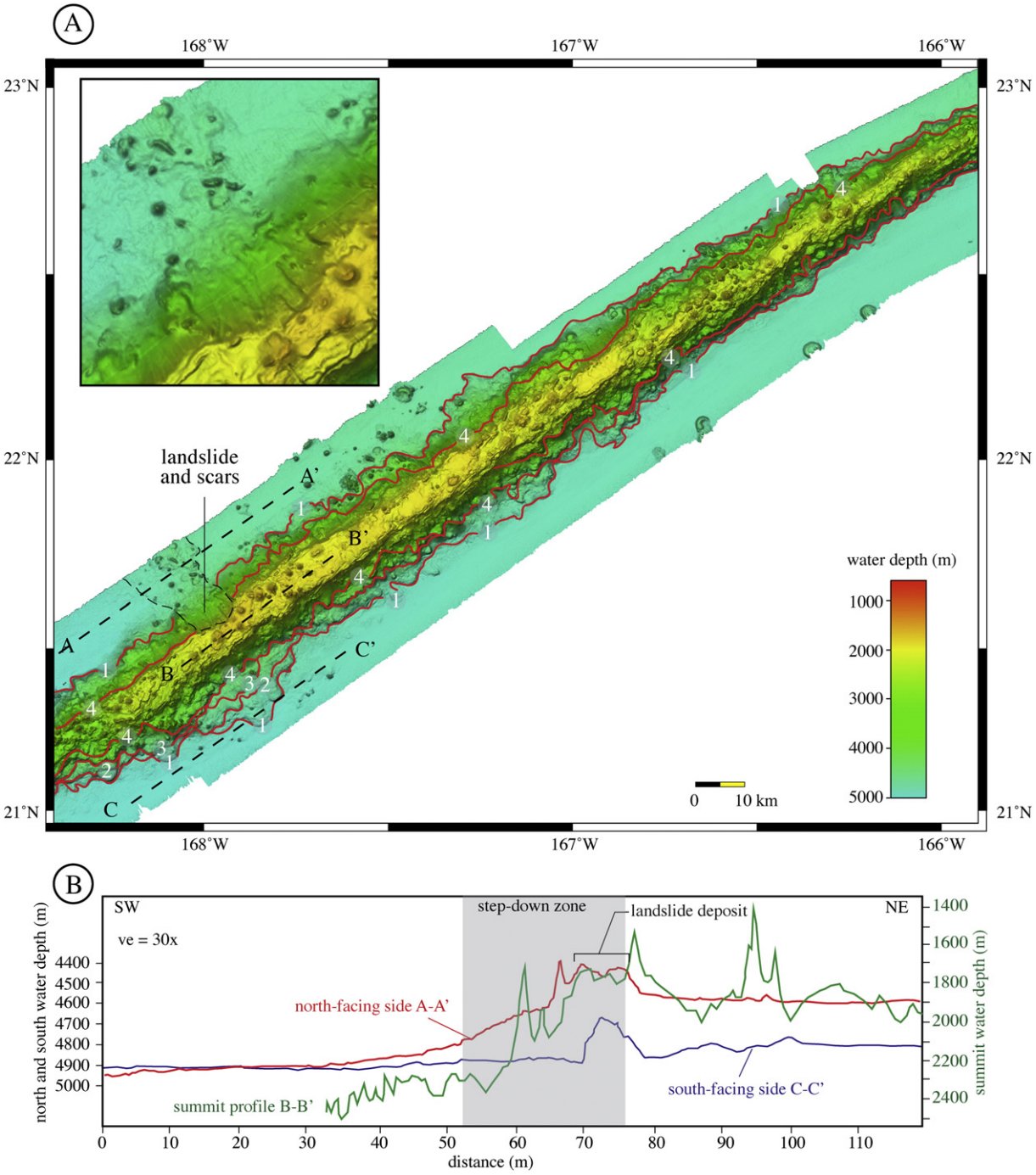

Fig. 10. (A) Map view of bathymetry of North Platform. Red numbered lines show extent of volcanic flows. The numbering continues from those in Fig. 10. Insert on upper left is close-up view of landslide and scars. (B) Profiles parallel to Necker Ridge showing the basin relief away from the northwest-facing (A–A′) and (C–C′) flanks as well as a crest profile (B–B′). The profiles illustrate the step-down in water depths at the location of a large landslide. (For interpretation of the references to color in this figure legend, the reader is referred to the web version of this article.)

are deeper than 4600 m, so the northeastern-most end of Necker Ridge is not exposed, although it is clear from the predicted bathymetry and GMTR grids that Necker Ridge does not project beyond the northeast side of Necker Island. The northern termini of four other linear ridges in the immediate vicinity are located close to, but not buried by, the archipelagic aprons of the Hawaiian Ridge (Fig. 1). The North Nose section ranges in width from 18.5 km at it southwest border with the North Platform section to 2.5 km wide in the extreme northeast. Flank slopes range from 13° to >20°. Water depths of the summit are ~2400 m on the southwest border with the North Platform section but begin a gradual deepening until at the northeastern tip where water depths are ~3500 m. The summit becomes more sharp-crested and narrower towards the northeast as it approaches Necker Island. The northern 50 km of the North Nose section is partially buried by an archipelagic apron shed off of the Hawaiian Ridge. The archipelagic apron has higher acoustic backscatter (−34 to −24 dB) than the abyssal seafloor (−40 to −38 dB) (Fig. 12B) and the area of higher backscatter is much more extensive on the north side of the ridge relative to the south side. There is a 400 m difference in water depth (northwest-facing side shallower than the southeast-facing side) that

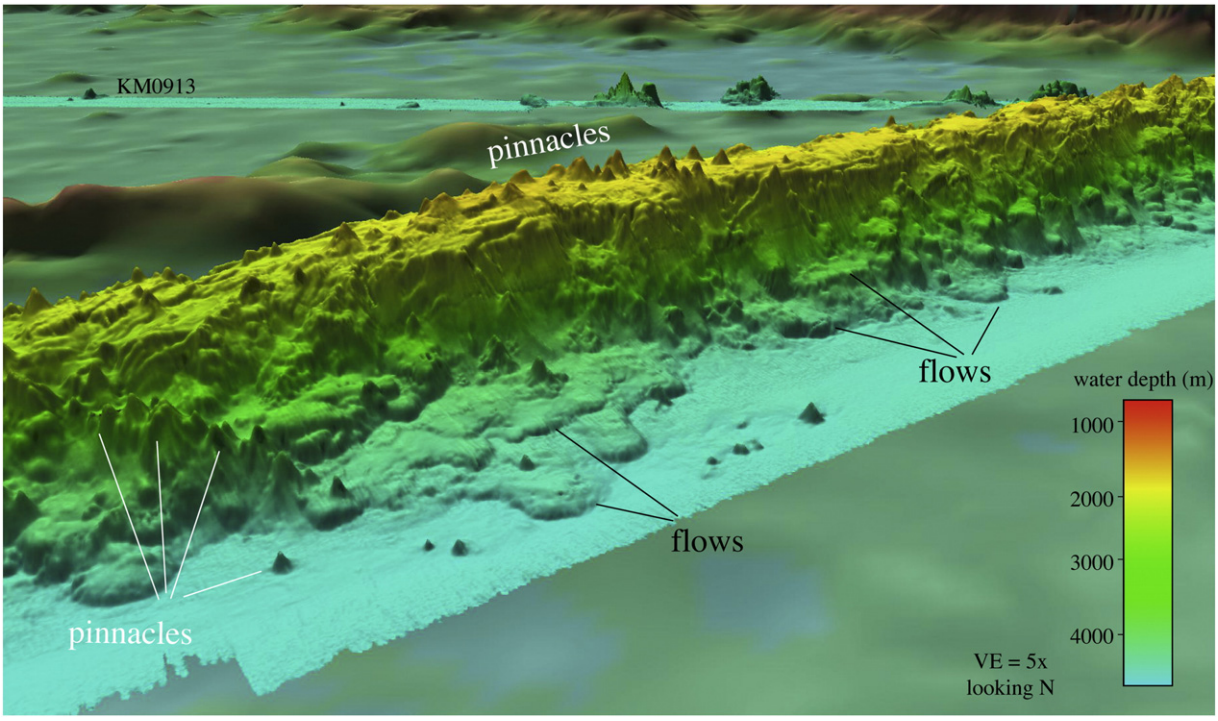

Fig. 11. Perspective view of bathymetry of North Platform showing examples of pinnacles and basal volcanic flows. KM0913 MBES line is shown in the upper background.

reflects a more extensive archipelagic apron on the north of the ridge. Distinct volcanic flows are not as clearly evident as are found to the southwest along the other sections of Necker Ridge.

North Nose has a distinct change in trend relative to the trend of most of Necker Ridge. Almost 600 km of Necker Ridge strikes N55E; however, beginning at 22.77°N/166.13°W the last 110 km (North Nose) strikes N65E (Fig. 12A dashed red lines). In addition, there are two cross-grains that strike across this section of the ridge; one trend is N82W and the other is N55W, the same trend as the main trend of Necker Ridge (Fig. 12A dashed white lines). The cross trends are marked by short 5 to 10 km long linear ridges that stand ~200 m above the general depth of the crest. The linear ridges are offset in an en echelon pattern that resembles the sides of a pull-apart basin (Fig. 12A white double arrow).

5. Discussion

5.1. Platforms and guyots

The region of Necker Ridge, the eastern Mid-Pacific Mountains and Horizon Guyot includes numerous guyots and five linear platforms (South Saddle platform, North and South Platforms on Necker Ridge and two platforms on Horizon Guyot). Conventional theories on the processes that formed the flat tops of the platforms and guyots include some combination of volcanism, erosion, reef formation, sedimentation, and subsidence (Winterer and Metzler, 1984; Moore et al., 1990; Clague et al., 2000; Eakins and Robinson, 2006, among many others). Unfortunately, drilling at DSDP Site 44 on Horizon Guyot (Fig. 1) sampled only part of the sediment section and did not reach basement. Horizon Guyot DSDP Site 171 (Fig. 1) is actually located at a 300 m deep saddle between two summit platforms so it did not sample the summit platform. The Horizon Guyot section at Site 171 recovered a Cretaceous (~99.6 Ma) basement of highly altered tholeiite basalts interbedded with shallow-water limestones and conglomerates (Winterer, 1973). In contrast, rocks dredged from the Mid-Pacific Mountains are alkalic basalts (Thiede et al., 1981), more typical of oceanic-island basalts. Basalts drilled at all sites on Horizon Guyot and the Mid-Pacific Mountains are overlain by a sequence of shallow-water limestones composed of algal-reef debris. The shallow-water facies is evidence that many of the guyots were at one time islands. The deposition of shallow-water limestones clearly occurred when these areas were near sea level prior to subsidence to the present depths of >2000 m. The subsidence at Horizon Guyot was reversed about 89 Ma and a recurrence of volcanism occurred for the next 5–23 Ma (Winterer, 1973). After the period of volcanism ended at ~66 Ma, this section of the ridge began a slow subsidence during which it accumulated 148 m of pelagic foram nanno ooze and chalk. The saddle area on Horizon Guyot at DSDP Site 171 is presently at a water depth of 2273 m. However, this same sequence of initial subsidence followed by uplift and then renewed subsidence apparently was not repeated in the Mid-Pacific Mountains (Winterer et al., 1973; Thiede et al., 1981).

The most distinctive morphological features of Necker Ridge are the two large elongate platforms (Fig. 14A, SP and NP) that morphologically resemble the two platforms of Horizon Guyot (Fig. 14A; HG-1 and HG-2) but they all reside at different water depths. So, what processes produced the flat platforms of Necker Ridge? Lonsdale et al. (1972) argued that the flat platform of Horizon Guyot (HG-1) was not the result of erosion at sea level but perhaps was the result of overlapping volcanic flows. However, DSDP Site 171 drilled on a saddle between HG-1 and HG-2 on Horizon Guyot and recovered a 173-m section of Cretaceous (100–110 Ma) lagoonal sediments at the basalt-sediment contact (Winterer et al., 1973). These results clearly demonstrate that Horizon Guyot was at or near sea level during the Cretaceous. Winterer and Metzler (1984) argued that because numerous reef rocks are found on the surfaces of many of the guyots of the Mid-Pacific Mountains, summit volcanic flows should be discounted as the explanation for these features. There are several guyots and flat-topped linear ridges in the region that have been partially mapped with multibeam echosounders so that some of their geomorphometrics can be compared to the completely mapped platforms of Necker Ridge. A plot of the general summit depths of these multibeam-mapped guyots and platforms is shown on Fig. 14B. South Platform (SP) has two summit platforms, an extensive southern section (SPs) with a mean depth of

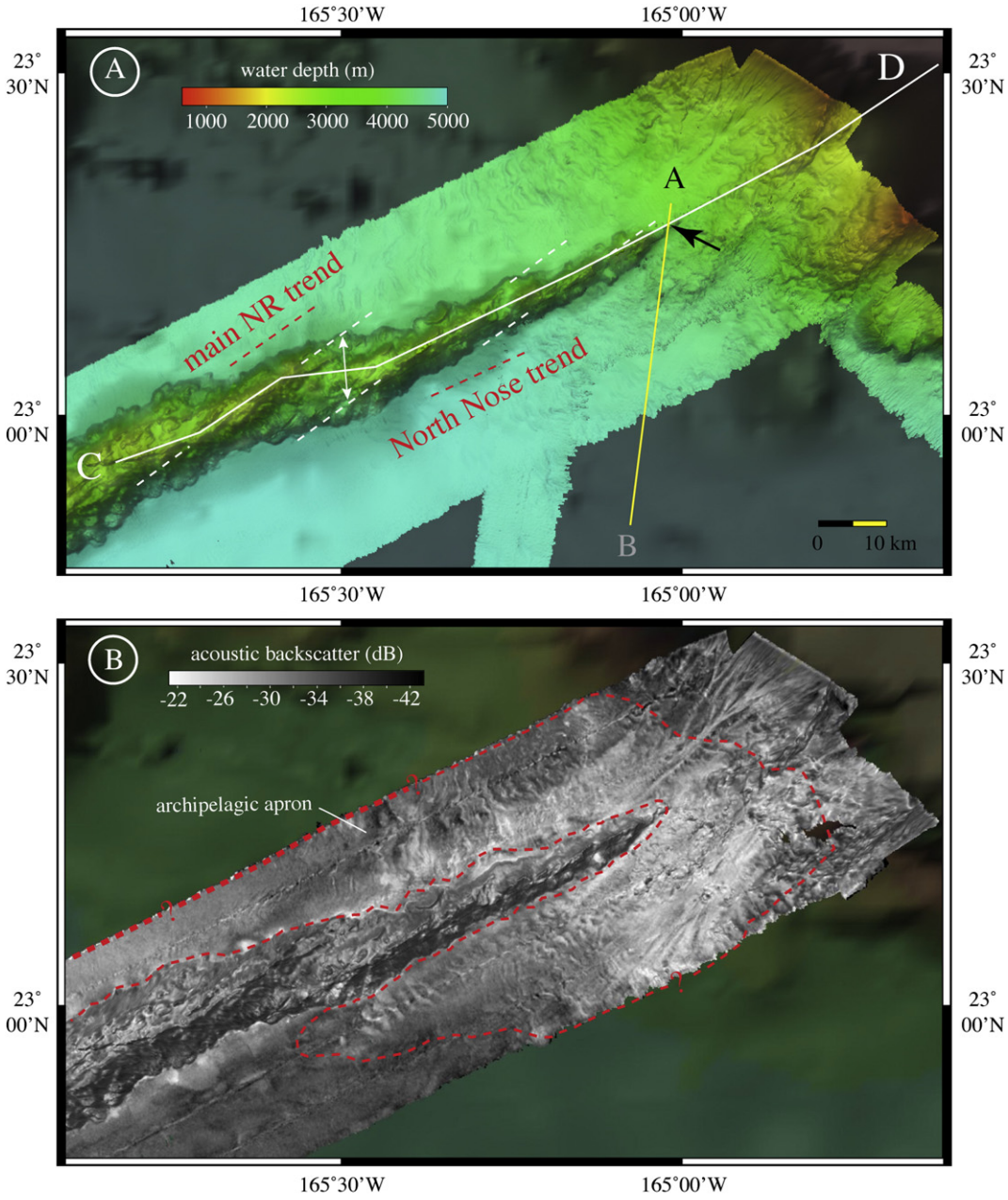

Fig. 12. (A) Map view of bathymetry of North Nose section. Red dashed lines show trend of the main Necker Ridge trend and the North Nose trend. White dashed lines show cross trends; white double arrow shows suggested pull-apart basin. Yellow line A–B is profile from the northern-most nose of unburied Necker Ridge to abyssal depths (see Fig. 14). White line is crest profile C–D of North Nose across the insular slope and onto the summit of Necker Island (see Fig. 14). Black arrow points to last exposure of Necker Ridge before being buried by the archipelagic apron of Necker Island. (B) Map view of acoustic backscatter of North Nose section showing the high acoustic backscatter (−26 to −22 dB) of the archipelagic apron (red dashed polygon) shed off of Necker Island. Bathymetry of the upper insular slope and Necker Island from Smith and Sandwell (1997, version 14.1). (For interpretation of the references to color in this figure legend, the reader is referred to the web version of this article.)

~2050 m and a much smaller northern section (SPn) at a mean depth of ~2250 m. Water depths of the summit of North Platform (NP) are ~1950 m but with a fairly large standard deviation ($2\sigma = 268$ m). The summit depths of the two relatively flat-topped platforms of Necker Ridge are a few hundred meters deeper than the depths of the poorly mapped relatively flat tops of nearby Horizon Guyot (HG-1 and HG-2) that stands at 1500–1850 m depths. The other guyots in the area (MP-1 through MP-6) are poorly mapped but single multibeam swaths across the summits of these guyots show water depths from 1200 to 2000 m. The relatively flat summits of the Mid-Pacific Mountain guyots suggest that at some time in the past the summit portion of the guyots and platforms was at sea level and that the entire region has since subsided nearly 2 km. However, the subsidence may not have been regional in scale, but perhaps was much more local. The eastern Mid-Pacific Mountains, just to the northwest of South Platform on Necker Ridge, was drilled at DSDP Site 313 (Fig. 1) at a sediment pond and recovered late Campanian (~70 Ma) volcanic sandstones and limestones lying on volcanic basement (Larson et al., 1975). Farther to the west of Necker Ridge in the western Mid-Pacific Mountains, DSDP Site 463 recovered Barremian (129–125 Ma) shallow-water clastic limestones that are evidence that this area was near sea level at that time (Thiede et al., 1981). Therefore, the range in summit depths may be the result of volcanism that varied along the length of Necker Ridge, Horizon Guyot and the eastern Mid-Pacific Mountains during the Middle to Late Cretaceous. The large variance in regional platform depths and basement ages suggests that the ridges that the platforms are built

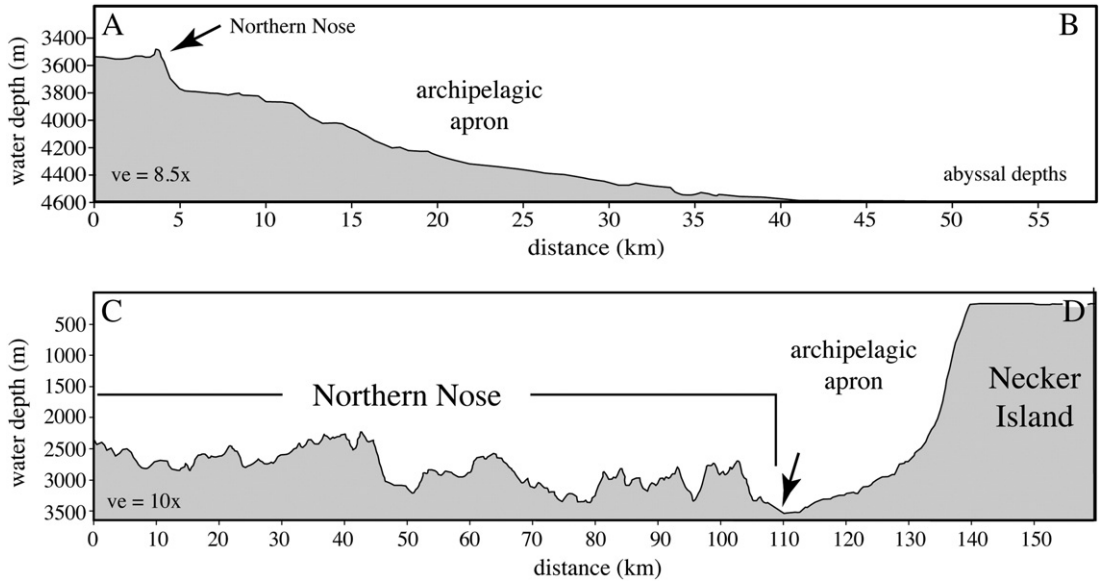

Fig. 13. (Upper) North–south Profile A–B from the archipelagic apron of Necker Island across the northern-most nose of unburied Necker Ridge to abyssal depths (see Fig. 13 for location). (Lower) Profile C–D along the crest of the Northern Nose of Necker Ridge (see Fig. 13 for location). Black arrow in both panels point to the northern-most nose of unburied Necker Ridge.

upon have undergone a complex history of construction and subsidence along their lengths. Only detailed sampling and dating can resolve the cause for the large variability in summit depths.

Winterer and Metzler (1984) (who did not have MBES data) discounted the flatness of the Mid-Pacific Mountains being caused by volcanic flows. However, from analyses of MBES data, this process was subsequently suggested by Clague et al. (2000) and Eakins and Robinson (2006) for the formation of flat-toped volcanic cones on the Hawaiian Ridge. The multibeam data of the present study clearly shows that the eastern Mid-Pacific Mountains, Necker Ridge and Horizon Ridge all have small volcanic features scattered on their flanks and summits that appear to be unrelated to the major flows that formed the ridges. These small volcanic features have been grouped here into a single class, called "pinnacles" (Figs. 4, 6 and 11) and may be similar to small-scale features from the Hawaiian Ridge that Clague et al. (2000) and Eakins and Robinson (2006) described as "pointed volcanic cones". Pinnacles on Necker Ridge rise from less than 100 to more than 400 m above the general depth of the flanks or summit platforms. Both conical-shaped and flat-topped pinnacles are common and some flat-topped pinnacles have a summit peak that rises an additional 20 to 80 m. The basal shapes of the pinnacles range from roughly circular to very elongate (1:4) but roughly circular pinnacles far outnumber elongate ones. The basal diameters of the pinnacles range from less than 1 km to more than 3.5 km. The flanks of some of the pinnacles along the length of Necker Ridge appear to be eroded and others show no indication of erosion, with no particular trend in occurrence. Mitchell and Lofi (2008) and Gardner (2010) used the degree of flank erosion to suggest relative age when comparing seamounts within an area. However, in the case of the pinnacles of Necker Ridge, the size of the pinnacles relative to the MBES footprint and resolution makes any quantitative determination problematic.

If the platforms of Necker Ridge received the same pelagic sediment that formed the thick sediment cover on the platforms at Horizon Guyot (Karig et al., 1970; Heezen et al., 1971; Lonsdale et al., 1972), then the pinnacles of the Necker Ridge platforms should have been buried if the pinnacles formed when the surfaces were close to sea level more than 70 Ma ago or if the pinnacles are related to late-stage main ridge-forming volcanism. The pinnacles cannot be patch reefs, as suggested by van Waasberger and Winterer (1993), because they occur at abyssal depths as well as being scattered throughout the vertical extent of Necker Ridge. Pinnacles on the platforms look no different than those on the lower flanks. Pinnacles on summit platforms may be pinnacle reefs that grew upward as the ridge subsided. However, those on the ridge flanks and abyssal seafloor are not pinnacle reefs because of their deep water depths even when the platforms were at sea level. The heights of the pinnacles seem too high to be pinnacle reefs and several of the pinnacles, especially on the area of North Platform, have cratered summits. The shape of the pinnacles, together with their occurrence on the ridge summits and the base of the ridge flanks, as well as the lack of burial by sediments, all suggest that these pinnacles are volcanic features that are not pinnacle reefs formed during the Middle Cretaceous and are much younger than the age of the formation of the ridges and the eastern Mid-Pacific Mountains.

The ability to correlate individual volcanic flows along trend for more than 600 km provides compelling evidence that the initial periods of volcanism were not spatially episodic along the length, such as occurs at a fracture zone (e.g., Pockalny et al., 1997; Eakins and Lonsdale, 2004), as might be inferred from the few basement ages. Instead, the apparent synchronous volcanism that occurred along a narrow 600+ km zone is evidence of a general trend of weakness in the Pacific Plate. The 10° splayed character of the 6 nearby linear ridges (Fig. 1) suggests that the weakness may have covered a large region of this part of the Pacific Plate.

There are three trends of cross grains along the length of Necker Ridge. Middle Saddle has a strong cross grain that strikes N30E whereas North Nose has two cross-grains that strike N82W and N55W. The bathymetric expression of the cross grains, and especially the separation between linear cross-grain ridges, has not been described in a mid-plate setting. Haxby and Weissel (1986), Winterer and Sandwell (1987) and Sandwell et al. (1995) describe cross grains of linear ridges formed on the oceanic crust of the Pacific Plate and attribute their formation to tensional cracks in the basement coupled with the rate of magma generation that expanded or closed the weaknesses. Their observed cross grains have wavelengths of 100 s of km, not 5 to 10 km as occurs on Necker Ridge. Perhaps the cross grains found in the Necker Ridge bathymetry are simply the finer-scale effects of the basement tensional cracks imaged by the higher resolution of the MBES that are interpreted from satellite altimetry (Haxby and Weissel, 1986; Sandwell et al., 1995) and seismic-reflection profiles (Winterer and Sandwell, 1987).

5.2. Pelagic sedimentation on Necker Ridge

Why is there so little pelagic sediment on the saddles between the platforms? The summits of the saddles have a lumpy morphological

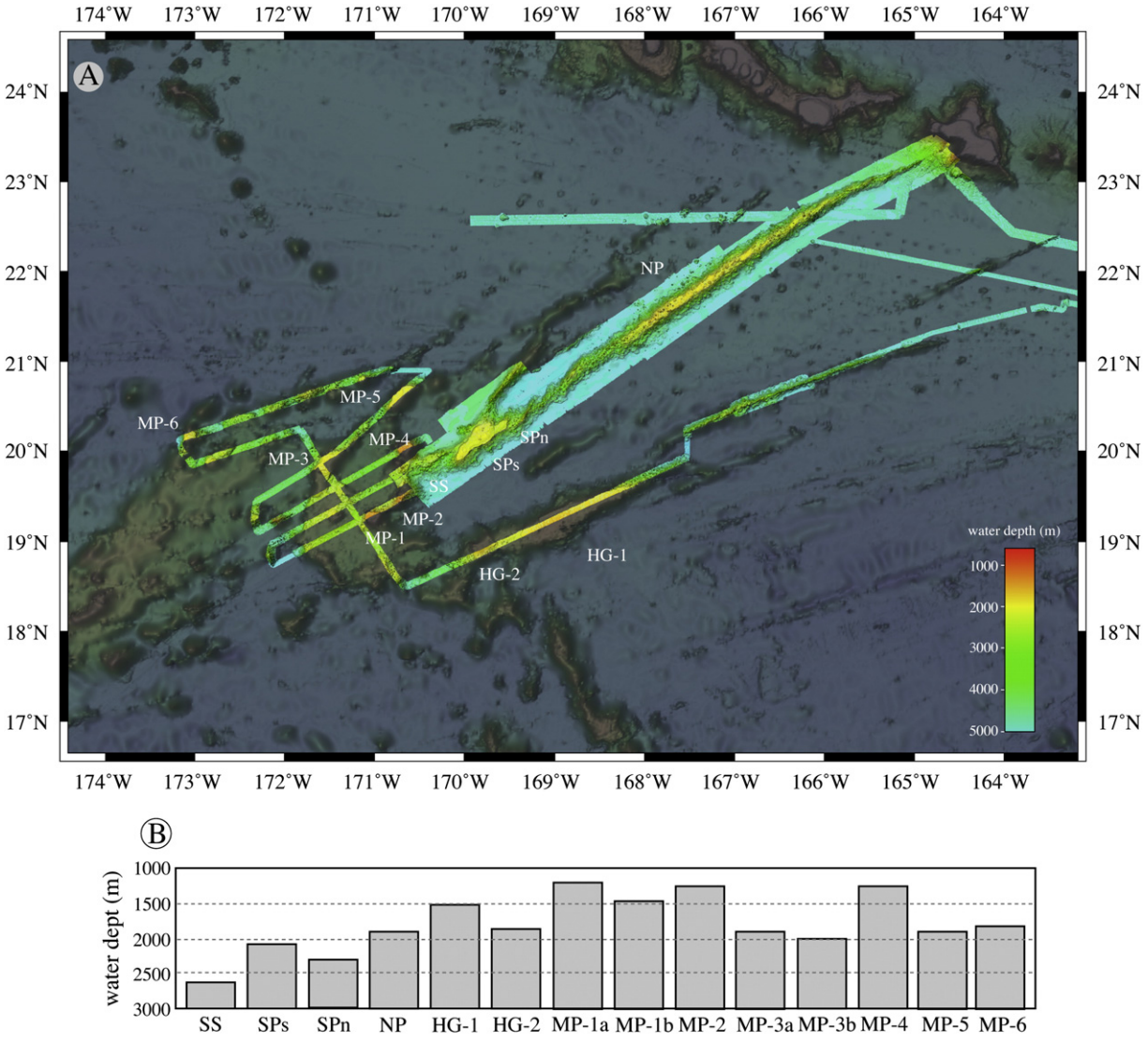

Fig. 14. (A) Composite map of MBES bathymetry from cruises KM0913, KM1121 and EX0909. Guyots mapped by MBES are indicated with white labels. (B) Plot of guyot summit depths: SS is Necker Ridge South Saddle; SPs is Necker Ridge main platform; SPn is Necker Ridge Lower Platform; NP is Necker Ridge North Platform; HG-1 is Horizon Guyot northern platform; HG-2 is Horizon Guyot southern platform; MP-1a through M-6 are guyots of the eastern Mid-Pacific Mountains. (For interpretation of the references to color in this figure legend, the reader is referred to the web version of this article.)

texture that is evidence of some sedimentation smoothing the relief of the flows, but not enough sediment thickness to completely smother the surface. Strong currents (>15 cm/s) have been measured on the summit of nearby Horizon Guyot (Lonsdale et al., 1972; Cacchione et al., 1988). Sediment cores from Horizon Guyot show evidence of winnowing of the finer fraction of the sediment. The measured currents and core samples from Horizon Guyot suggest that the surficial sediments from both Horizon Guyot and presumably Necker Ridge are presently being winnowed by deep-sea currents, but the samples demonstrate that the currents have not been strong enough to remove the coarser foraminiferal components from the platforms. Winterer (1973) discusses evidence from deep-sea drilling that suggests an increase in winnowing sometime during the past 10 Ma. Similarly, Karig et al. (1970) mention the same winnowed nature of sediments from the Mid-Pacific Mountains.

Pelagic sediments recovered at DSDP Site 171 on Horizon Guyot, 130 km south of Necker Ridge, range in age from Late Cretaceous (~70 Ma) to Holocene (Winterer et al., 1973). Average sedimentation rates are ~4 cm/ka for the 280 m of pelagic sediments that caps Horizon Guyot (Winterer et al., 1973). The water depths at the top of Horizon Guyot are within a few hundred meters of the summit depths of Necker Ridge, so that it is reasonable to assume that the same sedimentation rates apply to Necker Ridge. This area of the oceanic crust has migrated from a Mesozoic position at 16°S 130°W and crossed under the equatorial high-productivity zone and is now located at 20°N 169.5°W. Using the paleodepths of the carbonate compensation depth (CCD) of van Andel (1975), the portion of the Pacific Plate that Necker Ridge, Horizon Guyot and the eastern Mid-Pacific Mountains sit on has been above the CCD off and on for at least 35 Ma. Consequently, the ridges and Mid-Pacific Mountains should be buried under ~700 m of pelagic sediment, using a conservative average pelagic sedimentation rate of 2 cm/ka. Even winnowing 80% the sediment volume would produce ~140 m of sediment, enough sediment to blanket (and smooth) the saddles and ridge flanks. Yet the volcanic features are not buried under a thick sediment cover, so either the paleodepths of the CCD are in error or some other process has been active over the past 70 Ma to significantly reduce the amount of sediment that has accumulated on these bathymetric highs.

The saddles between the platforms on Necker Ridge, Horizon Guyot and areas of the eastern Mid-Pacific Mountains must represent areas of the seafloor that were below the photic zone during the initial formation of the two ridges whereas the platforms and guyots must have been elevated submarine highs or islands. The saddles must not

have been able to accommodate the colonization of corals whereas once the islands were eroded to sea level corals could build reefs to form the initial platforms. As subsidence progressed, the coral reefs kept pace with upward growth leaving the saddles with no possibility of coral colonization. However, if there is 150 + m of pelagic sediment above the shallow-water carbonates on the platforms, where is the pelagic sediment on the saddles? All of the saddles have been and still are at or above the lysocline (~3500 m) in this area (Peterson, 1966; Berger, 1967). Winnowing on Horizon Guyot apparently has only been efficient to erode clay and nannofossils but not the foraminifers. Certainly, the platforms are not below the CCD. It remains an enigma why the saddles are not buried by pelagic sediment.

5.3. Age of Necker Ridge

There is nothing in the MBES bathymetry or backscatter data that can indicate an age for Necker Ridge. However, the water depths of the top of Horizon Guyot are similar to the summit depths of Necker Ridge, so it is reasonable to assume that the average sedimentation rates at Horizon Guyot apply to Necker Ridge. If the age of Necker Ridge is on the order of 83 Ma (Saito and Ozima, 1977), then the top of Necker Ridge should be buried by ~450 m of pelagic sediments. If the age of Necker Ridge is ~77 Ma (Clague and Dalrymple, 1975), then the feature should be buried by ~425 m of sediment. However, if Necker Ridge is only ~10 Ma (Dalrymple et al., 1974), then the blanket of sediment should be only ~50 m thick. Drilling on Horizon Guyot penetrated 280 m of pelagic sediment and another 190 m of shallow-water limestone and basalt conglomerate (Winterer et al., 1973). The 280 + m of pelagic sediment at Horizon Guyot suggests that the Saito and Ozima (1977) age of 83 Ma for Necker Ridge is more reasonable than the other suggestions.

6. Conclusions

1. This study produced the first complete multibeam bathymetric map of Necker Ridge at a resolution of 100 m/pixel.
2. The bathymetry data show that Necker Ridge is constructed of a series of stacked volcanic flows, capped in two areas by thick carbonate platforms. Each flow is 200–400 m thick. The four oldest exposed volcanic flows can be followed for more than 600 km, indicating that the early volcanism occurred simultaneously along a long section of the seafloor and not in spatially separated areas along strike.
3. Scattered but numerous small conical volcanic pinnacles are found throughout Necker Ridge. The shape of the pinnacles, together with their occurrence on the ridge summits and the base of the ridge flanks, as well as their lack of burial by sediments, all suggest that these pinnacles are volcanic features that are not pinnacle reefs formed during the Middle Cretaceous and are much younger than the age of the formation of the ridges and the eastern Mid-Pacific Mountains.
4. Three summit platforms, presumed to have formed by shallow-water carbonates, are slightly tilted and asymmetric, in some areas to the NW and in other areas to the SE.
5. The northern section of Necker Ridge plunges to the NE and is buried by an archipelagic apron of the Hawaiian Ridge.
6. The relatively flat characteristics of the guyot summits suggest that at some time in the past the summit portion of the guyots and platforms were at sea level and that the entire region has since subsided nearly 2 km. However, the subsidence was not regional in scale, but much more local.
7. There is a conspicuous lack of pelagic sediment that should blanket the volcanic flows and the saddles between the summit platforms. This portion of the Pacific Plate has been above the CCD off and on for at least 35 Ma. Consequently, Necker Ridge should be buried under ~700 m of pelagic sediment, using a conservative pelagic sedimentation rate of 2 cm/ka. The saddles of Necker Ridge must have been below the photic zone during the initial formation whereas the two platforms of Necker Ridge must have been islands.
8. Based on pelagic sedimentation rates from a nearby DSDP site on Horizon Guyot and applied to Necker Ridge, the ~83 Ma age for the youngest volcanic flows on Necker Ridge as determined by Saito and Ozima (1977) appears to be reasonable.

Acknowledgments

We thank the officers, crews, technicians and watchstanders on the cruises of NOAA Ship *Okeanos Explorer* and RV *Kilo Moana*; without their efforts and cooperation the mapping would not have been accomplished. We especially want to thank Brian Taylor, Univ. of Hawaii for collecting the KM0913 multibeam line for us. Reviews of earlier drafts by Larry Mayer, Barry Eakins, Neil Mitchell and an anonymous reviewer were very constructive and much appreciated. The National Oceanic and Atmospheric Administration (NOAA) funded the EX0909 *Okeanos Explorer* cruise and the NOAA grant NA05NOS4001153 funded the KM1121 *Kilo Moana* cruise; both of which were in support of bathymetry mapping for the U.S. Extended Continental Shelf efforts. The U.S. bathymetry effort is unique among maritime nations in that the data collected have been available within a month or so after completion of each cruise (i.e., http://ccom.unh.edu/Law_of_the_sea.html; http://www.ngdc.noaa.gov/mgg/bathymetry/multibeam.html; http://www.geomapapp.org) for use by the scientific community and the public.

References

Atwater, T., Sclater, J., Sandwell, D., Severinghaus, J., Marlow, M.S., 1993. Fracture zone traces across the North Pacific Cretaceous Quiet Zone and their tectonic implications. In: Pringle, M.S., Sager, W.W., Sliter, W.V., Stein, S. (Eds.), The Mesozoic Pacific: Geology, Tectonics and Volcanism, Geophysical Monograph 77. American Geophysical Union, Washington DC, pp. 137–154.

Berger, W.H., 1967. Foraminiferal ooze: solution at depth. Science 156, 383–385.

Bridges, N.T., 1997. Characteristics of seamounts near Hawaii as viewed by GLORIA. Marine Geology 138, 273–301.

Cacchione, D.A., Schwab, W.C., Noble, M., Tate, G.B., 1988. Internal tides and sediment movement on Horizon Guyot, Mid-Pacific Mountains. Geo-Marine Letters 8, 11–17.

Chadwick Jr., W.W., Wright, I.C., Schwarz-Schampera, U., Hyvernaud, O., Reymond, D., de Ronde, C.E.J., 2008. Cyclic eruptions and sector collapses at Monowai submarine volcano, Kermadec arc: 1998–2007. Geochemistry, Geophysics, Geosystems. http://dx.doi.org/10.1029/2008GC002113.

Clague, D.A., Dalrymple, G.B., 1975. Cretaceous K–Ar ages of volcanic rocks from the Musicians seamounts and the Hawaiian ridge. Geophysical Research Letters 2, 305–308.

Clague, D.A., Moore, J.G., Reynolds, J.R., 2000. Formation of submarine flat-topped volcanic cones in Hawaii. Bulletin of Volcanology 62, 214–233.

Dalrymple, G.B., Lanphere, M.A., Jackson, E.D., 1974. Contributions to the petrology and geochronology of volcanic rocks from the leeward Hawaiian Islands. Geological Society of America Bulletin 85, 727–738.

Eakins, B.W., Lonsdale, P.F., 2004. Structural patterns and tectonic history of the Bauer microplate, eastern tropical Pacific. Marine Geophysical Researches 24, 171–205.

Eakins, B.W., Robinson, J.E., 2006. Submarine geology of Hana Ridge and Haleakala Volcano's northeast flank, Maui. Journal of Volcanology and Geothermal Research 151, 229–250.

Gardner, J.V., 2010. The West Mariana Ridge, western Pacific Ocean: geomorphology and processes from new multibeam data. Geological Society of America 122, 1378–1388.

Gardner, J.V., Mayer, L.A., Armstrong, A., 2006. Mapping supports potential submission to U.N. Law of the Sea. EOS, transactions. American Geophysical Union 87, 157–159.

Glass, J.B., Fornari, D.J., Hall, H.F., Cougan, A.A., Berkenbosch, H.A., Holmes, M.L., White, S.M., De La Torre, G., 2007. Submarine volcanic morphology of the western Galápagos based on EM300 bathymetry and MR1 side-scan sonar. Geochemistry, Geophysics, Geosystems. http://dx.doi.org/10.1029/2006GC001464.

Hamilton, E.L., 1956. Sunken islands of the Mid-Pacific Mountains. Geological Society of America Memoir 64, (97 pp.).

Haxby, W.F., Weissel, J.K., 1986. Evidence for small-scale mantle convection from Seasat altimeter data. Journal of Geophysical Research 91, 3507–3520.

Heezen, B.C., Fischer, A.G., Boyce, R.E., Bukry, D., Douglas, R.G., Garrison, R.E., Kling, S.A., Krasheninnikov, V., Lisitzin, A.P., Pimm, A.C., 1971. Initial Reports of the Deep Sea Drilling Project, v. 6. U.S. Government Printing Office, Washington D.C.(1329 pp.).

Hess, H.H., 1946. Drowned ancient islands of the Pacific basin. American Journal of Science 244, 772–791.

Karig, D.E., Peterson, M.N.A., Shor, G.G., 1970. Sediment-capped guyots in the Mid-Pacific Mountains. Deep-Sea Research 17, 373–378.

Larson, R.L., Moberly, R., Bukry, D., Foreman, H.P., Gardner, J.V., Keene, J.B., Lancelot, Y., Luterbacher, H., Marshall, M.C., Matter, A., 1975. Initial Reports of the Deep Sea Drilling Project, v. 32. U.S. Government Printing Office, Washington D.C.(980 pp.).
Lonsdale, P., Normark, W.R., Newman, W.A., 1972. Sedimentation and erosion on Horizon Guyot. Geological Society of America Bulletin 85, 289–316.
Mark, R.K., Moore, J.G., 1987. Slopes of the Hawaiian Ridge. In: Decker, R.W., Wright, T.L., Stauffer, P.H. (Eds.), Volcanism in Hawaii. U.S. Geological Survey Professional Paper, v. 1350. U.S. Government Printing Office, Washington, D.C., pp. 101–107.
Menard, H.W., 1984. Origin of guyots: beagle to seabeam. Journal of Geophysical Research 89, 11,117–11,123.
Mitchell, N.C., Lofi, J., 2008. Submarine and subaerial erosion of volcanic landscapes: comparing Pacific Ocean seamounts with Valencia Seamount, exposed during the Messinian Salinity Crisis. Basin Research 20, 489–502.
Moore, J.G., 1987. Subsidence of the Hawaiian Ridge. In: Decker, R.W., Wright, T.L., Stauffer, P.H. (Eds.), Volcanism in Hawaii. U.S. Geological Survey Professional Paper, v. 1350. U.S. Government Printing Office, Washington, D.C., pp. 85–100.
Moore, J.G., Campbell, J.F., 1987. Age of tilted reefs, Hawaii. Journal of Geophysical Research 92, 2641–2646.
Moore, J.G., Clague, D.A., Ludwig, K.R., Mark, R.K., 1990. Subsidence and volcanism of the Haleakala Ridge, Hawaii. Journal of Volcanology and Geothermal Research 42, 273–284.
Müller, R.D., Roest, W.R., Royer, J.-Y., Gahagan, L.M., Sclater, J.G., 1997. Digital isochrons of the world's ocean floor. Journal of Geophysical Research 102, 3211–3214.
Peterson, M.N.A., 1966. Calcite: rates of dissolution in a vertical profile in the Central Pacific. Science 154, 1542–1544.
Pike, R.J., 1995. Geomorphometry — progress, practice and prospect. Zeitschrift für Geomorphologie, Supplementband 101, 221–238.
Pockalny, R.A., Fox, P.J., Fornari, D.J., Macdonald, K.C., Perfit, M.R., 1997. Tectonic reconstruction of the Clipperton and Siqueiros Fracture Zones: evidence and consequences of plate motion change for the last 3 Myr. Journal of Geophysical Research 102, 3167–3181.
Ryan, W.B.F., Carbotte, S.M., Coplan, J.O., O'Hara, S., Melkonian, A., Arco, R., Weissel, R.A., Ferrini, V., Goodwille, A., Nitsche, F., Bonczkowski, J., Zemsky, R., 2009. Global multi-resolution topography synthesis. Geochemistry, Geophysics, Geosystems. http://dx.doi.org/10.1029/2008GC002332.
Saito, K., Ozima, M., 1977. $^{40}Ar/^{39}Ar$ geochronological studies of submarine rocks from the western Pacific area. Earth and Planetary Science Letters 33, 353–367.
Sandwell, D.T., Winterer, E.L., Mammerickx, J., Duncan, R.A., Lynch, M.A., Levitt, D.A., Johnson, C.L., 1995. Evidence for diffuse extension of the Pacific plate from Pukapuka ridges and cross-grain gravity lineations. Journal of Geophysical Research 100, 15,087–15,099.
Smith, W.H.F., Sandwell, D.T., 1997. Global seafloor topography from satellite altimetry and ship depth soundings. Science 277, 1957–1962.
Thiede, J., Dean, W.E., Rea, D.K., Vallier, T.L., Adelseck, C.G., 1981. The geologic history of the Mid-Pacific Mountains in the central North Pacific Ocean — a synthesis of deep-sea drilling studies. In: Thiede, J., Vallier, T.L., et al. (Eds.), Initial Reports of the Deep Sea Drilling Project, v. 62. U.S. Government Printing Office, Washington D.C., pp. 1073–1120.
van Andel, T.H., 1975. Mesozoic/Cenozoic calcite compensation depth and the global distribution of calcareous sediments. Earth and Planetary Science Letters 26, 187–194.
van Waasberger, R.J., Winterer, E.L., 1993. Summit geomorphology of western Pacific guyots. In: Pringle, M.S., Sager, W.W., Sliter, W.V., Stein, S. (Eds.), The Mesozoic Pacific: Geology Tectonics and Volcanism. American Geophysical Union Monograph, 77. American Geophysical Union, Washington D.C., pp. 335–366.
Vogt, P.R., Smoot, N.C., 1984. The Geisha Guyots: multibeam bathymetry and morphometric interpretation. Journal of Geophysical Research 89, 11,085–11,107.
Ware, C., Knight, W., Wells, D., 1991. Memory intensive statistical algorithms for multibeam bathymetric data. Computers & Geosciences 17, 985–993.
Wessel, P., Kroenke, L.W., 1997. A geometric technique for relocating hotspots and refining absolute plate motions. Nature 387, 365–369.
Winterer, E.L., 1973. Regional problems. In: Winterer, E.L., Ewing, J.I., et al. (Eds.), Initial Reports of the Deep Sea Drilling Project, v. 17. U.S. Government Printing Office, Washington D.C., pp. 911–922.
Winterer, E.L., Metzler, C.V., 1984. Origin and subsidence of guyots in Mid-Pacific Mountains. Journal of Geophysical Research 89, 9969–9979.
Winterer, E.L., Sandwell, D.T., 1987. Evidence from en-echelon cross-grain ridges for tensional cracks in the Pacific plate. Nature 329, 534–537.
Winterer, E.L., Ewing, J.I., Douglas, R.G., Jarrard, R.D., Lancelot, Y., Moberly, R.M., Moore, T.C., Roth, P.H., Schlanger, S.O., 1973. Initial Reports of the Deep Sea Drilling Project, v. 17. U.S. Government Printing Office, Washington D.C., pp. 283–334.